Open Ceramics 9 (2022) 100206

Contents lists available at ScienceDirect

Open Ceramics

journal homepage: www.sciencedirect.com/journal/open-ceramics

Solid solution enhanced electrostriction in the YSZ-GDC system

Veronica Chierchia [a], Haiwu Zhang [b], Mauro Bortolotti [a], Andrea Chiappini [c], Gian D. Sorarù [a], Vincenzo Esposito [b], Mattia Biesuz [a,*]

[a] University of Trento, Department of Industrial Engineering, Via Sommarive 9, 38123, Trento, Italy
[b] Technical University of Denmark (DTU), Department of Energy Conversion and Storage, Fysikvej, 2800, Kongens Lyngby, Denmark
[c] Institute of Photonics and Nanotechnologies (IFN-CNR) CSMFO Laboratory and Fondazione Bruno Kessler (FBK) Photonics Unit, 38123, Trento, Italy

ARTICLE INFO

Keywords:
Electrostriction
YSZ
GDC
Solid solution
Fluorite
Electromechanics

ABSTRACT

Giant electrostrictors based on oxygen deficient fluorites are of great technological and scientific interest due to their unusual electromechanical properties. It is, however, still not clear whether solid solutions between different fluorites can affect the electrostrictive properties.

In this work, we investigated the electromechanical response of four different solutions of 10 mol% gadolinium-doped ceria (GDC10) and 8mol% yttria-stabilized zirconia (8YSZ), corresponding to 1, 5, 10 and 20 wt% of 8YSZ into GDC10. An increase in the electrostriction coefficient with the 8YSZ content (maximum between 10 and 20 wt%) was registered. This effect suggests that the development of complex solid solutions could represent a new tool to develop electromechanical materials with superior properties.

1. Introduction

Materials developing mechanical stresses in response to the application of an external electric field are of great relevance for a wide range of applications, including actuators, transducers, micro-, nano-electromechanical systems, pumping devices for Biomed etc. However, traditional electromechanical materials (EMM), i.e., piezoelectrics, are based on Pb-containing perovskites, are toxic and dangerous for human health and the environment. In such a context, the research of novel and high-performance Pb-free EMM is a timely challenge.

It has been recently shown that some oxygen-deficient fluorites (ODF) possess exceptional electrostrictive properties that are even superior to the best performing Pb-based piezos [1–3]. Among them, gadolinium-doped ceria (GDC) displays an unusual electrostriction coefficient, M_{33}, (i.e., the ratio between the electromechanic strain, x_3, and the square of the electric field amplitude, E_3^2, with $x_3 = M_{33} E_3^2$), which surpasses by 2–3 orders of magnitude the one predicted by classical Newnham's electromechanical theory [4,5]. As such, Gd-doped CeO_2 can develop stress of more than 500 MPa, which is way higher than the value reached by the piezoelectrics and electrostrictors currently in use [1].

Such unusual properties were attributed to a change in bond lengths in the vicinity of the oxygen vacancies (abundantly present in GDC due to gadolinium doping) [6,7]. Thus, it is assumed that electrostriction strongly depends on the configuration of the oxygen vacancies and the presence of cations-vancacy pairs, e.g. the $M'_{Ce} - v^{\cdot\cdot}_{O}$ dipole [8]. This configuration depends on the size [9] and valence of the dopants, which reflects the elastic and electrostatic interactions between the cation and the vacancy [3]. Moreover, it has been shown that giant electrostriction seems to be a common property shared by different fluorite-structured oxides possessing a large number of oxygen vacancies, including also δ-Bi_2O_3 [4].

Albeit giant electrostriction is a common feature in oxygen-deficient fluorites, it is still unknown how the electrostriction coefficient would change when different fluorites are mixed into a solid solution. This work aims at providing a first preliminary report on the electromechanical properties of fluorites, namely YSZ and GDC, solid solutions.

2. Materials and methods

GDC10 (Treibacher) and 8YSZ (TZ-8YS, Tosoh) commercial powders were used. Different mixtures were produced, corresponding to 0, 1, 5, 10, 20, and 100 wt% of YSZ.

Firstly, a slurry was created by mixing the 20 g powder with deionized water (72.9 vol%) and 0.5 vol% of a dispersant (Darvan 821A). The slurry was ball milled for 2 h in a high-energy mixer (Turbula, T2F) along with some alumina spheres (about 30 g). Then, the alumina spheres were removed from the slurry and added 8.5 vol% of a

* Corresponding author.
E-mail address: mattia.biesuz@unitn.it (M. Biesuz).

https://doi.org/10.1016/j.oceram.2021.100206
Received 30 September 2021; Received in revised form 1 December 2021; Accepted 6 December 2021
Available online 7 December 2021

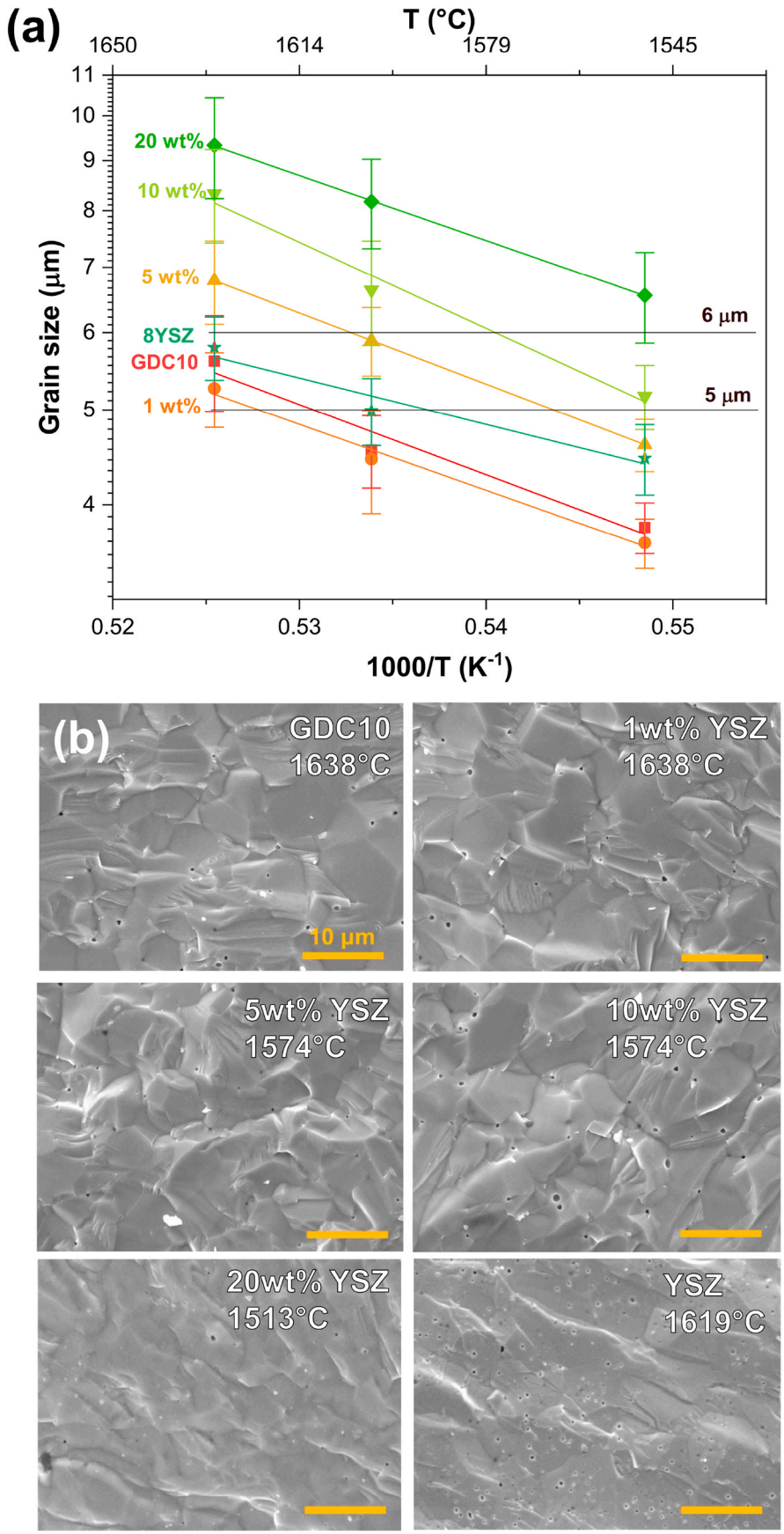

Fig. 1. (a) Arrhenius plot of grain size (G) concerning the sintering temperature for different solid solutions. (b) SEM micrographs of the fresh fracture surface of the ceramics sintered at the selected temperatures.

Table 1
Sample label, sintering temperature, cell parameter and electrostriction coefficient for materials containing various YSZ contents.

Sample label	Sintering temperature (°C)	Cell parameter (Å)	M_{33} at 10 Hz (10^{-18} m^2 V^{-2})
GDC10	1638	5.418(2)	2.3±0.1
1 wt%	1638	5.412(6)	2.8±0.6
5 wt%	1574	5.399(3)	19.0±0.5
10 wt%	1574	5.385(1)	21.2±0.5
20 wt%	1513	5.346(0)	55.0±3
8YSZ	1619	5.143(7)	≈0.1

binder (Duramax B1014). The compound was then dried on a Petri dish under a fume cupboard on a heating plate set at 60 °C.

After drying, the 0.3 g of powder was uniaxially pressed in a steel die (8 mm diameter) under 200 MPa. As the microstructural differences between the samples could change the electromechanical properties [10], a preliminary microstructural investigation was carried out on the different compositions to obtain materials with comparable grain size. The samples were sintered in a muffle furnace at 1550, 1600, and 1630 °C (dwell at the sintering temperature = 2 h). The sintered samples were polished and thermally etched at 1350 °C for 30 min and observed by SEM JEOL JSM5500. The average grain size dimension was calculated by following the ASTM E112 Norm [11] (Fig. 1(a)). Subsequently, different sintering temperatures (Table 1) were selected for each composition to get solid solutions with grain size approximatively between 5 and 6 μm.

The sintered samples were characterized by XRD using an IPD3000 ItalStructures diffractometer equipped with a Co-kα source and Inel CPS120 detector. Their fresh fracture surface was investigated by SEM (JEOL JSM5500), and the density was measured by Archimede's method using an analytical balance with sensitivity ±0.1 mg. Raman spectra were obtained using a LabRAM Aramis equipped with an excitation laser 532 nm. EDXS maps were also acquired to check the homogeneity of the material.

Before the electromechanical testing, the samples were polished with SiC sandpapers and a 1 μm diamond suspension. Then, a gold electrode 150 nm thick was deposited on the polished side of the pellets through the thermal evaporation technique (Inficon, XTM/2). Finally, the samples were attached to an alumina support by applying a thin layer of silver ink on the unpolished side (creating the second electrode) and connected to Cu wires. A SIOS Meβtechnik laser interferometer equipped with a UHL Technische Mikroskopie microscope and a National Instrument proximity sensor was used to perform the electromechanical measurements. The core of the vibrometer was a Michelson interferometer with a laser wavelength of 632 nm (resolution = 5 pm). The

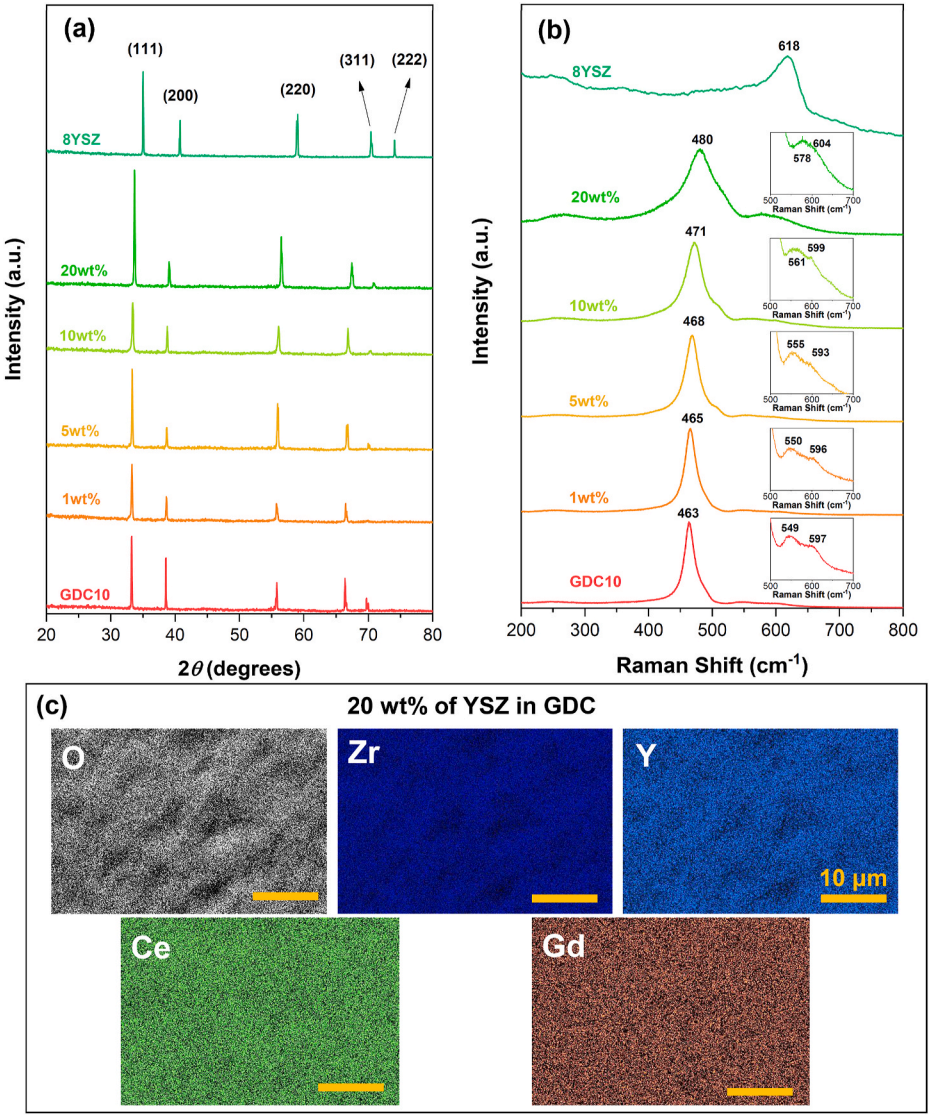

Fig. 2. (a) XRD and (b) Raman spectra of samples containing different YSZ content; (c): elemental EDXS maps obtained on the sample containing 20 wt% of YSZ.

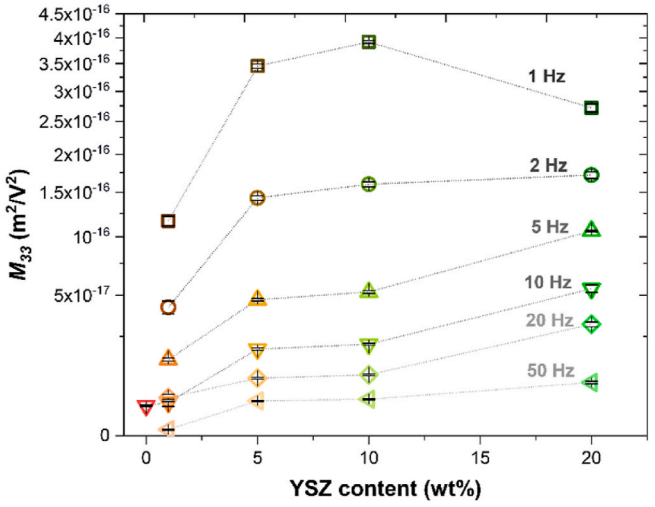

Fig. 3. M_{33} at different frequencies for various YSZ-GDC solid solutions.

voltage (0 – 800 V) was applied by the mean of a TGP3112 Aim TTi generator combined with a 2220 TREK amplifier. Finally, a 7230DSP lock-in amplifier by Ametek Signal Recovery was used for signal acquisition.

3. Results and discussion

The relative density of the solid solutions sintered at the selected temperatures always exceeded 97% of the theoretical one. The high level of densification is further confirmed by the SEM micrographs in Fig. 1(b), which also point out the presence of large micrometric grains. The diffractograms of the sintered materials (Fig. 2(a)) point out that, in all the cases, a single-phase fluorite-type solid solution was obtained, whose cell parameter depends on its composition (Table 1). The unit cell tends to shrink as the YSZ content increases due to the lower ionic radius of Zr^{4+} for Ce^{4+}. No secondary phases were detected. The EDXS maps further confirm the formation of a homogeneous solid solution (Fig. 2 (c)) in the material containing the highest "solute" (YSZ) concentration (20 wt%) and sintered at the lowest temperature (1513 °C).

The Raman spectra of GDC and YSZ (Fig. 2(b)) show the typical vibrational transitions associated with fluorites [12,13]. The main peak is located at 463 and 618 cm^{-1} for GDC and YSZ, respectively, and is associated with the symmetric stretching of the MO_8 cubes [12]. The feature shifts and broadens when increasing the YSZ content in GDC, pointing out an effective dissolution of the solute leading to an increase in the structural disorder of the system. Two additional features of the GDC spectrum at 549 and 597 cm^{-1} can be attributed to extrinsic, $(Gd'_{Ce} - v_O^{\cdot\cdot})^{\cdot}$ and intrinsic, $(Ce'_{Ce} - v_O^{\cdot\cdot})^{\cdot}$ defect clusters, respectively [12]. Whereas the intrinsic high-frequency feature marginally shifts with the YSZ doping, the extrinsic one moves toward a higher wavenumber increasing the YSZ content in the solid solution. This effect suggests that the Zr^{4+} cations are preferentially accommodated in the vicinity of the oxygen vacancies bonded to the trivalent dopants (i.e., Gd^{3+}), whereas they marginally interact with vacancies bonded to Ce^{3+}. It is also possible to observe that the ≈550 and 600 cm^{-1} features increase with the YSZ content in the composites suggesting a higher degree of $M'_{Ce} - v_O^{\cdot\cdot}$ association [8].

The electromechanical response of GDC10 and YSZ samples was compatible with the literature ($M^{GDC}{}_{33}$ ≈10^{-18} and $M^{YSZ}{}_{33}$≈10^{-19} m^2V^{-2} at 10 Hz). Interestingly, the electrostriction coefficient of the solid solutions (Fig. 3 and Table 1) resulted way larger than that of the pure GDC and YSZ, reaching a maximum of 55 x 10^{-18} m^2V^{-2} (10 Hz) in the material containing 20 wt% of YSZ (≈20 times larger than that of pure GDC). This trend is substantially confirmed at different frequencies (Fig. 3), though at low frequency (1 Hz) the highest electromechanical response is achieved with a lower doping level (10 wt% of YSZ). On the other hand, M_{33} increases monotonically within the selected compositional range (0–20 wt% of YSZ) for frequencies > 5Hz (at 2 Hz it seems to reach a saturation between 10 and 20 wt%). This effect suggests that further optimization of the electromechanical properties of the solid solution is possible by adding larger amounts of YSZ, especially in the "high frequency" region, which are of particular relevance in several technological devices.

The reasons behind the observed behavior deserve further investigations to elucidate the mechanistic effect of the solid solution on electrostriction. However, the obvious modification of the chemical environment of the oxygen vacancies detected by Raman spectroscopy (Fig. 2(b)) seems to be the most reasonable origin. Giant electrostriction in oxygen-deficient fluorites originates from the lattice deformation in the vicinity of the oxygen vacancies, which can interact with the elastic deformation of the lattice due to the presence of ions in a solid solution.

Despite being preliminary, these results definitively show that giant electrostriction of solid solutions is not "averaged" over the solid solution components, thus providing a new tool to enhance the electromechanical response of oxygen-deficient fluorites. Further investigations are needed to elucidate better the effect of the solid solution on the chemical environment of oxygen vacancies and its relation with giant electrostriction. We especially envision that X-ray near-edge absorption spectroscopy or *in-situ* Raman spectroscopy would clarify the key mechanisms of aliovalent cations-vacancies pairs on the electromechanical properties.

4. Conclusions

The electromechanical response of homogeneous GDC-YSZ solid solutions (0–20 wt% of YSZ) increases with the YSZ content, reaching a maximum between 10 and 20 wt% of YSZ depending on the analyzed frequency. An electrostriction coefficient as high as 55 x 10^{-18} m^2V^{-2} was measured at 10 Hz in the solid solution containing 20 wt% of YSZ, whereas values exceeding 10^{-16} m^2V^{-2} were achieved at 1 Hz. Although the origin of this solid solution-enhanced giant electrostriction is not clear yet, it is suggested to be linked to a change of the chemical environment around the oxygen vacancies detected by Raman spectroscopy.

Declaration of competing interest

The authors declare that they have no known competing financial interests or personal relationships that could have appeared to influence the work reported in this paper.

Acknowledgments

This work was supported by the "JECS Trust" [Contract No.2020242]; and "Fondazione Caritro (Cassa di Risparmio di Trento e Rovereto)" [Innovative processing routes to green high entropy ceramics with enhanced functional properties (HiEnCer) project]. VIES thanks the European Union's Horizon 2020 research and innovation programme under Grant Agreement No. 801267 (BioWings) for partially supporting this work.

References

[1] R. Korobko, A. Patlolla, A. Kossoy, E. Wachtel, H.L. Tuller, A.I. Frenkel, I. Lubomirsky, Giant electrostriction in Gd-doped ceria, Adv. Mater. 24 (2012) 5857–5861, https://doi.org/10.1002/adma.201202270.
[2] N. Yavo, O. Yeheskel, E. Wachtel, D. Ehre, A.I. Frenkel, I. Lubomirsky, Relaxation and saturation of electrostriction in 10 mol% Gd-doped ceria ceramics, Acta Mater. 144 (2018) 411–418, https://doi.org/10.1016/j.actamat.2017.10.056.
[3] A. Kabir, V. Buratto Tinti, M. Varenik, I. Lubomirsky, V. Esposito, Electromechanical dopant–defect interaction in acceptor-doped ceria, Mater. Adv. 1 (2020) 2717–2720, https://doi.org/10.1039/D0MA00563K.

[4] N. Yavo, A.D. Smith, O. Yeheskel, S.R. Cohen, R. Korobko, E. Wachtel, P.R. Slater, I. Lubomirsky, Large nonclassical electrostriction in (Y, Nb)-Stabilized δ-Bi2O3, Adv. Funct. Mater. 26 (2016) 1138–1142, https://doi.org/10.1002/adfm.201503942.
[5] R.E. Newnham, V. Sundar, R. Yimnirun, J. Su, Q.M. Zhang, Electrostriction: nonlinear electromechanical coupling in solid dielectrics, J. Phys. Chem. B 101 (1997) 10141–10150, https://doi.org/10.1021/jp971522c.
[6] A. Kossoy, Y. Feldman, R. Korobko, E. Wachtel, I. Lubomirsky, J. Maier, Influence of point-defect reaction kinetics on the lattice parameter of Ce 0.8 Gd 0.2 O 1.9, Adv. Funct. Mater. 19 (2009) 634–641, https://doi.org/10.1002/adfm.200801162.
[7] R. Korobko, A. Lerner, Y. Li, E. Wachtel, A.I. Frenkel, I. Lubomirsky, In-situ extended X-ray absorption fine structure study of electrostriction in Gd doped ceria, Appl. Phys. Lett. 106 (2015), https://doi.org/10.1063/1.4906857, 042904.
[8] S. Santucci, H. Zhang, A. Kabir, C. Marini, S. Sanna, J.K. Han, G. Ulbrich, E. M. Heppke, I.E. Castelli, V. Esposito, Electromechanically active pair dynamics in a Gd-doped ceria single crystal, Phys. Chem. Chem. Phys. 23 (2021) 11233–11239, https://doi.org/10.1039/D1CP00748C.
[9] M. Varenik, J.C. Nino, E. Wachtel, S. Kim, S.R. Cohen, I. Lubomirsky, Trivalent dopant size influences electrostrictive strain in ceria solid solutions, ACS Appl. Mater. Interfaces 13 (2021) 20269–20276, https://doi.org/10.1021/acsami.0c20810.
[10] A. Kabir, S. Santucci, N. Van Nong, M. Varenik, I. Lubomirsky, R. Nigon, P. Muralt, V. Esposito, Effect of oxygen defects blocking barriers on gadolinium doped ceria (GDC) electro-chemo-mechanical properties, Acta Mater. 174 (2019) 53–60, https://doi.org/10.1016/j.actamat.2019.05.009.
[11] A. I, E112 Standard Test Methods for Determining Average Grain Size, 2010.
[12] S.A. Acharya, V.M. Gaikwad, V. Sathe, S.K. Kulkarni, Influence of gadolinium doping on the structure and defects of ceria under fuel cell operating temperature, Appl. Phys. Lett. 104 (2014), 113508, https://doi.org/10.1063/1.4869116.
[13] M.A. Borik, S.I. Bredikhin, V.T. Bublik, A.V. Kulebyakin, I.E. Kuritsyna, E. E. Lomonova, P.O. Milovich, V.A. Myzina, V.V. Osiko, P.A. Ryabochkina, N. Y. Tabachkova, Structure and conductivity of yttria and scandia-doped zirconia crystals grown by skull melting, J. Am. Ceram. Soc. 100 (2017) 5536–5547, https://doi.org/10.1111/jace.15074.